J. Chem. Lett. 4 (2023) 117-129

Research Article

Journal of Chemistry Letters
journal homepage: www.jchemlett.com
ISSN (online) 2717-1892 (print) 2821-0123

Synthesis and Application of TiO_2-Phosphomolybdic acid nanocomposite.

Praveendaniel M[1], Rajesh Anantha Selvan P[1]

[1]*Research scholar (Reg.No-20111272031005, Department of chemistry, St. John's College, Palayamkottai, Tirunelveli, Tamil Nadu, Affiliated to Manonmaniam Sundaranar University, Tirunelveli. India*
[1]*Department of chemistry, St. John's College, Palayamkottai, Tirunelveli, Tamil Nadu, Affiliated to Manonmaniam Sundaranar University, Tirunelveli. India*

ARTICLE INFO

Article history:
Received 3 May 2023
Received in revised form 11 July 2023
Accepted 15 July 2023
Available online 10 August 2023

Keywords:
Nanocomposite
TiO_2 doped with Phosphomolybdic acid
Antimicrobial activity
Photodegradation,

ABSTRACT

TiO_2 doped with phosphomolybdic acid composites were synthesized by the blending method. The above prepared TiO_2-phosphomolybdic acid composites were characterized by UV-visible, FT-IR, XRD, SEM and EDAX methods. Photocatalytic degradation efficiency also studied. The UV-visible spectra showed a strong peak for the base TiO_2 and doped phosphomolybdic acid and the absorption spectra indicate a decrease in band-gap energy upon doping, and with slight increase in Urbach energy. FT-IR structural features reveal the peak of TiO_2, phosphomolybdic acid and TiO_2-phosphomolybdic acid composite peaks. The XRD study proved that there was a slight decrease in the particle size in the composite materials. SEM study also showed that a decrease in particle size and uniform distribution of dopant. Heber multi lamp photo-reactor visible light irradiation of Methylene blue (MB) dye was effectively degraded. The antibacterial effect against *Streptococcus mutans* was examined using the disc diffusion method. This was shown to be effective against antibiotics and Streptococcus mutans.

1. Introduction

Nanocomposites are composite materials that are made up of two or more components, in which at least one should be nanoscale in size. These materials offer unique properties due to their size and Structure[1]. The nanoscale components are usually combined with a larger scale materials such as polymers, ceramics, or metals to create a material with superior properties compared to their individual components[2]. Nanocomposites have been used in a variety of applications, such as electronics, aerospace, biomedical, and energy[3]. In the research paper, the study on nanocomposites is to revolutionize existing technologies or to enable new one entirely[4].

TiO_2 nanocomposites are a type of nanomaterial that combine titanium dioxide (TiO_2) with other materials such as polymers, metals, or semiconductors, in order to create materials with enhanced properties. As TiO_2 is an easily applicable chemical, these nanocomposites are suitable for high refractive index, high chemical resistance and high ultraviolet (UV) durability[5]. Furthermore, the nanocomposites are utilized for a wide range of applications including photocatalysis, antimicrobial, gas sensing, and solar cells. The combination of TiO_2 with other materials can result of materials with improved properties such as increased optical transparency, better thermal stability, and enhanced electrical conductivity.

The addition of TiO_2 nanoparticles to polymers can significantly improve their mechanical properties such as tensile strength and modulus, which improve the performance of mechanical properties. TiO_2 nanoparticles can act as a thermal stabilizer, which result improved thermal stability and better performance even in high temperature applications. Adding TiO_2 nanomaterials with any other materials improve the electrical conductivity of the composite material. The TiO_2 based nanocomposite are used to fill the micro-cracks and voids of the composite material, and to provide a better electrical pathway for the flow of

∗ Corresponding author. e-mail: rajesh.chem@stjohnscollege.edu.in
https://doi.org/ 10.22034/JCHEMLETT.2023.395693.1114

electrons. Inclusion of TiO_2 nanoparticles can improve the surface properties of polymers, such as surface roughness and wettability. The cost of TiO_2 nanocomposites is lower than other materials, as TiO_2 is affordable. TiO_2 nanocomposite perform cost-effective solutions for so many applications.

TiO_2 doped with Phosphomolybdic acid nanocomposites is a type of nanomaterial which is composed of a combination of titanium dioxide (TiO_2) and phosphomolybdic acid (PMA). TiO_2 is a common semiconductor material while PMA is an inorganic acid[6]. These nanocomposites have been used in various applications such as dye-sensitized solar cells, photocatalytic degradation of organic pollutants, and water purification. They have also been used as a coating material for protecting surfaces from corrosion and used as a catalyst for the production of polymers[7]. These nanocomposites offer a wide range of advantages, such as high stability, high efficiency, and low cost. Additionally, they have excellent optical, electrical, and mechanical properties.

TiO_2 is a photocatalyst which is widely used in many industrial and environmental applications. PMA is a heteropoly acid (HPA) that possesses numerous qualities, such as strong acidity, chelating ability, and catalytic activity[8]. The combination of TiO_2 and PMA in a composite material provides numerous advantages. For example, the PMA can enhance the photocatalytic activity of TiO_2 by providing an electron acceptor, while the TiO_2 can improve the ability of transportation of electron and stability of the PMA[9]. Furthermore, the combination of the two materials can improve the surface area and higher catalytic activity.

TiO_2 doped with phosphomolybdic acid nanocomposites have been studied for their potential antimicrobial activities. The nanocomposites are synthesized using a simple and cost-effective technique, and their efficacy is evaluated using the disc diffusion method. The disc diffusion method is a qualitative method used to evaluate the antimicrobial activity of a substance observing the zone of inhibition around the discs impregnated with the sample. The size of the zone of inhibition is compared to control and determine the antimicrobial activity of the sample. The aim of this study is to investigate the antimicrobial effect of TiO_2 doped phosphomolybdic acid nanocomposite against various bacterial species. The result obtained from the disc diffusion method will be used to evaluate the potential of TiO_2 nanocomposites doped with phosphomolybdic acid used as an antimicrobial agent[10].

Characterization of TiO_2 nanocomposites involves various techniques such as (UV-Vis, FTIR, XRD, SEM with EDAX, Photodegradation studies) UV-Visible spectroscopy is used to determine the optical properties of TiO_2 nanocomposites, such as band gap energy and absorption spectra. FTIR spectroscopy is used to determine the chemical composition of the nanocomposites, while X-ray diffraction is used to analyze the crystallinity of the nanocomposites. Scanning electron microscopy-energy dispersive X-ray spectroscopy is used to analyze the microstructure of the nanocomposites and to determine the elemental composition. Photodegradation studies are used to investigate the photocatalytic activity of the nanocomposites. Finally, antimicrobial activity tests are used to evaluate the potential of the nanocomposites for antimicrobial applications. By using these techniques, the structure and properties of TiO_2 nanocomposites can be studied in detail, which will help to development a new and improved materials.

2. Experimental Part

2.1 Material's

The chemicals used in this works are available commercially and are being used. TiO_2 has been obtained from Loba Chemicals and it has no gas and assuredness. Hydrochloric acid and Sodium hydroxide pellets were purchased from Spectrum chemicals. Phosphomolybdic acid was brought in analytical regent from SRL Pvt. Ltd. Heteropoly acid (HPA) is a doping material that is Phosphomolybdic acid. Methylene blue dye was purchased from Himedia ltd.

2.2 Synthesis of Nanocomposites

The blending method is a simple method that was used for nanocomposites. TiO_2 of 1g and various concentrations of phosphomolybdic acid were blended in a motor for 60 minutes. The blended composites were heated in an air oven at 110ºC for 30 minutes. Similarly, different samples 2, sample 3, sample 4 and sample 5 by milling various concentrations of 0.01M, 0.001M, 0.05M, and 0.005M of phosphomolybdic acid respectively were used for sample preparation.

2.3 Characterization Methods

Several characterization methods have been devised to investigate the size, shape, surface analysis, and the distribution of nanocomposites in different environments. Here, we discuss the main techniques for the characterization of the UV-visible spectrum of TiO_2 doped with Phosphomolybdic acid composites were recorded on Shimada Zu UV-Vis spectrometer. Estimate their band gap energy by UV-vis spectrophotometer. The functional group analysis by FT-IR spectrometer 8400 S was recorded in the wavenumber range 400-4000 cm^{-1} and with 2 cm^{-1} resolution through Shimadzu and the electronic spectra spectrophotometer. For X-Ray diffraction, the XRD patterns were recorded by Philips model x pert pro diffractometer through Cu-Kα radiation at λ=1.1556Å, using a generator voltage of 40Kv and

current 40mA, and the scanning range 2θ and 10 to 80º with 0.025º degree. SEM studied by using SEM instrument for 4th generation scanning electron microscope with FEG Schottky electron emission source which combines SEM imaging and live elemental composition analysis in a single window of TESCAN'S VEGAS-3. Even though TiO_2 nanoparticles were imaged with SE detector for 10 keV, TESCAN'S VEGAS-3 high and low vacuum SEM analysis operations instrument was equipped with energy dispersive X-ray analyzer EDAX and then further studying by elemental mapping.

2.4 Photocatalytic degradation of Methylene Blue

Photocatalytic experiments were performed in a photocatalytic reactor. Dye solutions containing the photocatalyst were placed in borosilicate reactor tubes and aerated for 30 minutes to reach equilibrium[11]. The reactor tubes were then placed in the reaction chamber and the solutions were subjected to irradiation at 365 nm for 3h. During the reaction, samples of the dye solution were collected at intervals of each 10 minutes, 20 minutes, 30 minutes, 40 minutes, 50 minutes, 60 minutes, 120 minutes and 180 minutes. Eventually, the extent of degradation was measured by using an Optical Density measuring UV-vis spectrophotometer model 6300PC. The percentage of degradation efficiency (η) was calculated according to the following equation[12].

$$\eta = C_t - C_o / C_t \times 100 \qquad (1)$$

where C_o is the initial concentration of Methylene Blue, and C_t is the concentration of Methylene Blue after time t.

2.5 Antimicrobial activity

The antimicrobial activity of TiO_2 doped with phosphomolybdic acid against Streptococcus pyogenes (MTCC 442) has been studied. The method involves using agar, a type of culture medium which contains an antibiotic and TiO_2 doped with phosphomolybdic acid nanocomposites. The test microorganisms were added to the agar and incubated at 37°C for 48 hours. After the incubation, the results were recorded. The results indicates that the TiO_2 doped with phosphomolybdic acid have antimicrobial activity against Streptococcus pyogenes. Therefore, TiO_2 doped with phosphomolybdic acid allows Streptococcus pyogenes to grow strongly. As amoxicillin has antimicrobial, it don't permit the bacteria to grow. These antimicrobial activity exists in TiO_2 doped with phosphomolybdic acid.

3. RESULT AND DISCUSSION

3.1 UV-Vis Analysis

The spectral properties of the base TiO_2 and TiO_2 doped phosphomolybdic acid nanocomposites were studied by recording the UV-vis absorbance spectra in the wavelength range 200-800nm. Fig.1. TiO_2 was considered as main spectrum, which is compared to other reflectance of spectrums b, c, d and e. The indirect band-gap energies of the base TiO_2 and TiO_2 doped phosphomolybdic acid nanocomposites were obtained from Tauc plots of $(\alpha h\nu)2(eVcm^{-1})^2$ vs. Energy (h*ν*) derived from as it is shown in Table 1. In Tauc plots of $(\alpha h\nu)2(eVcm^{-1})^2$, The UV-DRS Tauc plot equation $(\alpha h\nu)2(eVcm^{-1})^2$ is used to represent the relationship between the absorption coefficient (α) of a material, the incident photon energy (hν), and the energy of the absorbed photon (eV). This equation can be used to analyze the optical properties of a material, such as its absorption, transmission, and reflection characteristics. It can also be used to calculate the absorption coefficient at different photon energies, which can be used to estimate the efficiency of the materials. The band gaps were evaluated as 3.20, 2.86, 2.68, 2.23 and 2.79eV for the TiO_2 and Sample 2, 3, 4 and 5 respectively. The band gaps describe the composite, created in the crystal lattice caused by doping. Which affect the real band-gap energy and Urbach energy, which is found through '$\alpha=\alpha_0 \exp E/E_u$'. where α is the absorption coefficient, E is the photon energy, and E_u is the band-gap energy and Urbach energy This energy has been determined from the slope of the linear portion of the graph between lnα vs photon energy below the band gap energy as shown in Fig. 2. Since the absorption coefficient is proportional to F(R), the term α can be replaced by F(R). The band-gap energy can be obtained by observing the way of slope from linear fittings of plots. It can be observed that the band-gap energy is higher for the doped samples than TiO_2 due to an increase in oxygen vacancies. The absorption spectrum of TiO_2 nanocomposites exhibits an absorption onset at 352 nm. After doping with Phosphomolybdic acid, the absorption onset is shifted slightly and wavelength has changed(Fig. 1b to e). This red shift may be attributed to decreases the band gap for the TiO_2 nanocomposites. Therefore, as Phosphomolybdic acid exists in TiO_2 doped with Phosphomolybdic acid it is found that the band gap has been decreased in other four samples.

The TiO_2-doped with phosphomolybdic acid band-gap energy values are determined by the type of dopant and the concentration of dopant. The Urbach energy values are determined by the material's structural disorder. The higher the Urbach energy, the more disorder there is within the material, which affects the band-gap energy[13]. Therefore, the TiO_2-doped phosphomolybdic acid band-gap energy values are larger than the Urbach energy values due to the dopant increasing the material's band gap. The difference between band-gap energy and Urbach energy is that band-gap energy is the energy required to create an electron-hole pair, while Urbach energy is

the energy required to change the width of the band gap. Band-gap energy values are typically much larger than Urbach energy values.

Table 1. UV-Vis spectra of band gap energies as well as the Urbach energies

Sample	UV-Vis peaks (nm)	Band gap Energy (eV)	Urbach Energy (meV)
TiO_2	350	3.20	0.93
Doped Sample (0.01M)	352	2.86	0.27
Doped Sample (0.001M)	354	2.68	0.47
Doped Sample (0.05M)	358	2.23	0.40
Doped Sample (0.005M)	356	2.79	0.31

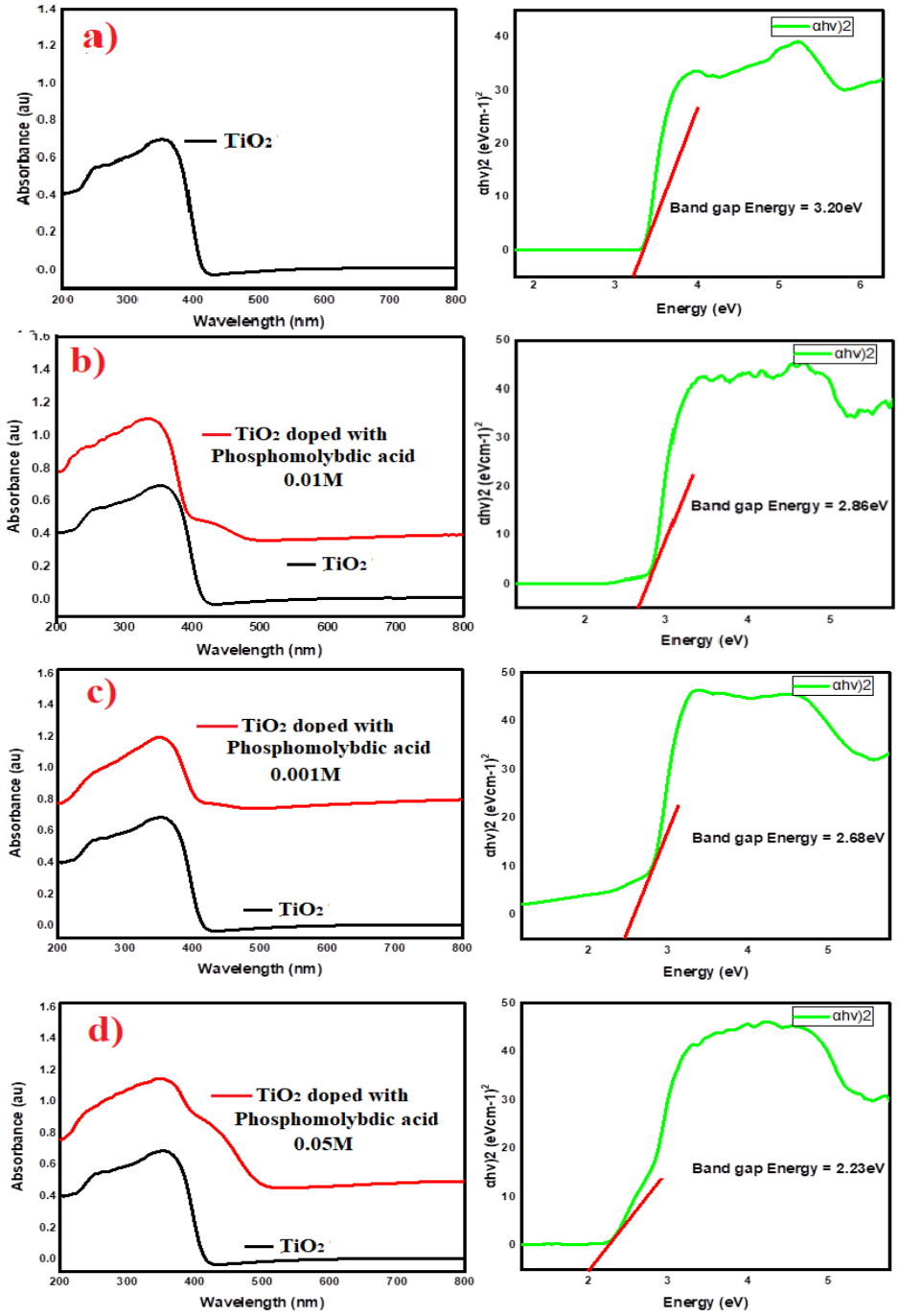

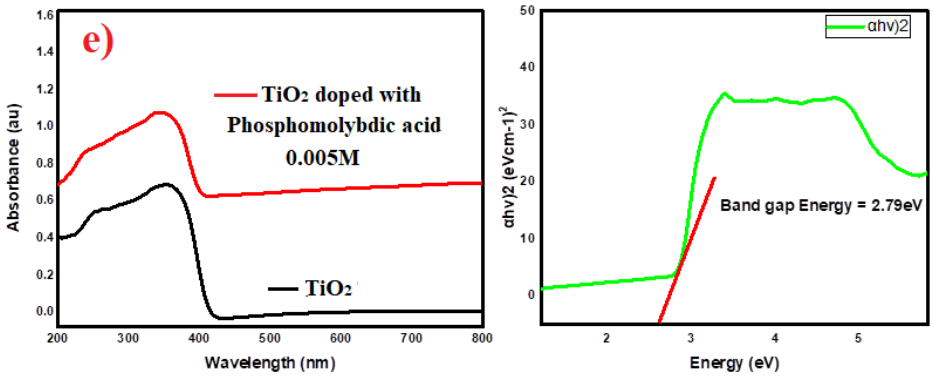

Fig.1. UV-Vis Tauc Plot absorption spectrum of TiO_2 and TiO_2 doped with phosphomolybdic acid nanocomposite

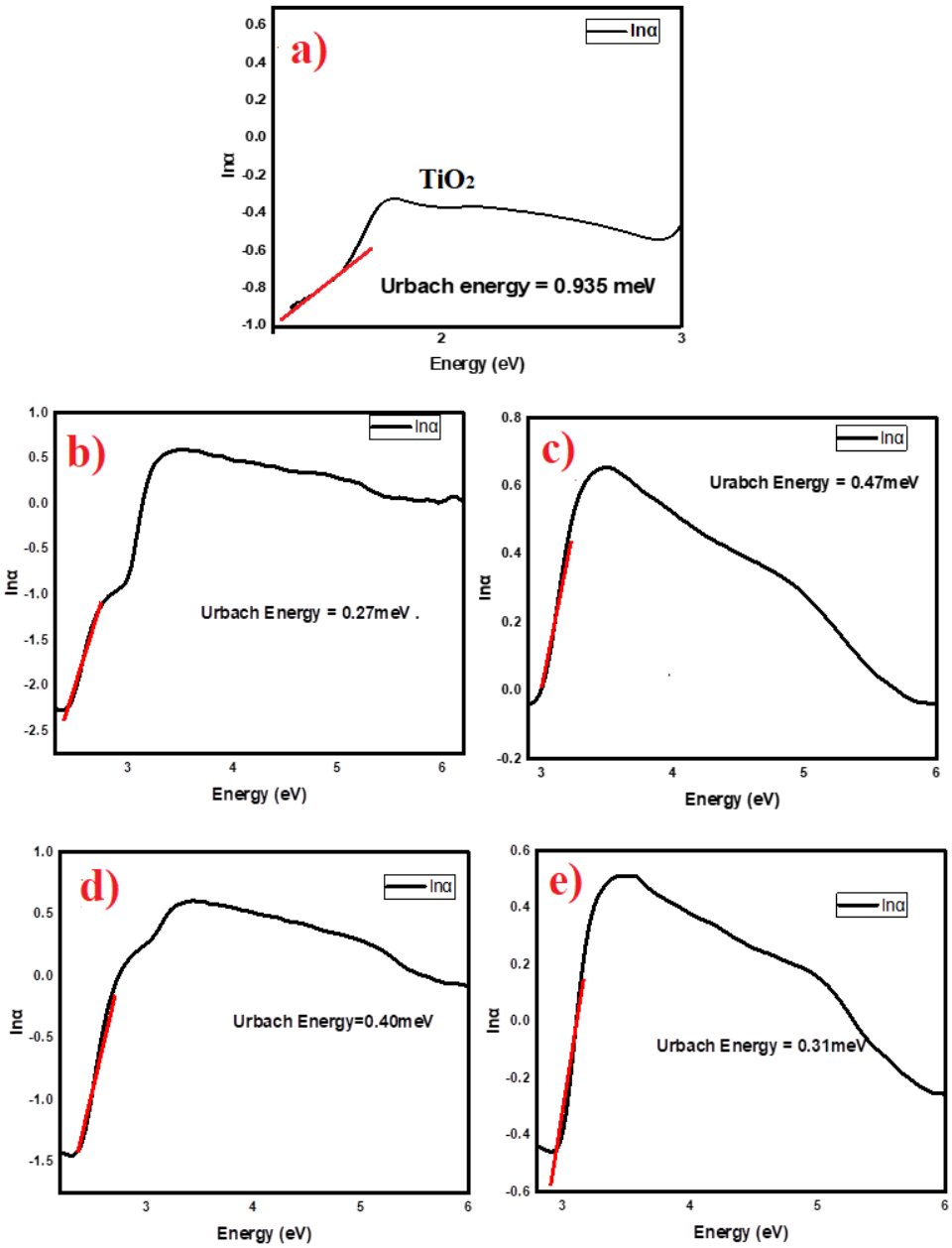

Fig.2. UV-Vis Urbach energy absorption spectrum of TiO_2 and TiO_2 doped phosphomolybdic acid nanocomposite

3.2 FT-IR Spectra

The FT-IR spectra of TiO_2 nanocomposite samples are shown in Fig.3. Metal and its composites have small change in peaks or bands including in position and intensities. In Pure TiO_2, the characteristic absorption bands are found as 3566, 2932, 1601, 1387, 1067 and 620 cm^{-1}. The 3566 cm^{-1} absorption band is attributed to the stretching of O-H bonds in water molecules adsorbed on the surface of the TiO_2. The 2932 cm^{-1} absorption band is attributed to stretching of C-H bonds in hydrocarbons[14-15]. The 1601 cm^{-1} absorption band is attributed to O-H bending in water molecules. The 1387 cm^{-1} absorption band is attributed to the stretching of Ti-O bonds. The 1067 cm^{-1} absorption band is attributed to the bending of Ti-O bonds. The 620 cm^{-1} absorption band is attributed to the bending of Ti-O-Ti bonds[16]. The characteristics of the composites of sample 2 peak at about 3580, 2906, 1618, 1378, 1071 and 655cm^{-1}. These frequencies represent the different bonds present in the nanocomposite material. Peaks at 3580 cm^{-1} peak corresponds to the stretching vibration of O-H bonds, the 2906 cm^{-1} peak represents the C-H stretching vibration, the 1618 cm^{-1} peak is attributed to C=C bonds, the 1378 cm^{-1} peak is attributed to the vibration of C-O bonds, the 1071 cm^{-1} peak is attributed to the vibration of P=O bonds and the 655 cm^{-1} peak is attributed to the vibration of Ti-O bonds. All the characteristics of sample 2 to sample 5 peak are shifted slightly in TiO_2-doped phosphomolybdic acid nanocomposite, and indicating that there is a strong interaction between those two components. The spectra of sample 3 possess the following peaks at 3584, 2910, 1373, 1080 and 703cm^{-1}. The peak at 703cm^{-1} is assigned to the stretching mode of P-O bond, 1373 cm^{-1} to M=O terminal bond and finally 617cm^{-1} to C-H out plane bending vibration metal oxide[17]. Therefore, the above results show that Phosphomolybdic acid (PMA) is certainly interacting with TiO_2 and form the new composites. In sample 4 shifted vibrations of composites are observed that from 1101 to 617cm^{-1} M=O bond of Phosphomolybdic acid and O-Ti-O bend from 2932cm^{-1}. Eventually, the same change occurred in sample 5. Thus the interaction of Phosphomolybdic acid composite with confirmed.

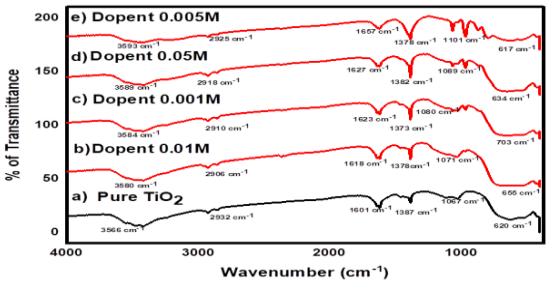

Fig.3. FTIR spectrum of Pure TiO_2 and TiO_2 doped with phosphomolybdic acid Nanocomposites

3.3. XRD patterns

The crystal structures and phase purities of the base TiO_2 and nanocomposites such as sample 2, sample 3, sample 4 and sample 5 were analyzed by powder X-ray diffractograms. Entire peaks, in the XRD patterns could be of Phosphomolybdic acid and were in good accordance with the reported standard (JCPDS No.89-6975). The reflection planes are considered as the monoclinic phase of the TiO_2 Fig.4. Thus, XRD characterization not only proved the presence of each component but also their interaction and the amorphous or crystalline nature. The XRD patterns showed in (Fig.4a) amorphous peaks of pure TiO_2 as (100), (002), (112), (020), (120), (202), (002), (311) planes, and (011), (200), (222), (211), (230), (321), (214), (032), and (132) of TiO_2 doped with Phosphomolybdic acid as (Fig.4.b). The peaks were in the agreement with the wurtzite hexagonal structure (JCPDS file no. 89-6975 and 39-0026) of the phosphomolybdic acid nanocomposite[18]. The crystallites size (D) of the nanocomposites was calculated using by the Debye -Scherrer formula:

$$D=\frac{0.9\lambda}{\beta\ Cos\theta} \qquad (2)$$

There, β is the full-width at half maximum (FWHM) in the peaks, θ is the diffraction angle, and λ is the X-ray wavelength(1.5406Å). In the research, the Williamson Hall plot method is an important tool which was used to characterize nanocomposites of TiO_2 and Phosphomolybdic acid. The method is generally used to determine the crystallite size, stress and strain of the nanocomposite material.

(Fig.4) The Williamson Hall plot is based on the Bragg's law of diffraction, which states that the angular position of the diffraction peak is inversely proportional to the size of the crystal lattice[19]. Moreover, the method is used to find the smaller crystallite, and of the higher diffraction peak. The Williamson Hall plot method consists of plotting the diffraction peak position (2θ) on the x-axis and of the peak width (FWHM) on the y-axis.

The line, connecting the data points, is known as the Williamson Hall plot[20].

The slope of the line is related to the strain in the material, while the intercept is related to the crystallite size and stress. By analyzing the Williamson Hall plot, it is possible to determine the strain, crystallite size, and stress of the TiO_2 nanocomposite as shown in Fig.5. The average crystallite size was calculated as given in the Table 2. The Micro strain (ε) values 1.04, 0.83 ,1.96, 0.39 indicate that the material consists of a range of crystallite sizes spread across the plotted range, from small to large.

The higher the strain value, the larger the crystallite size. Therefore, the values 1.04, 0.83, 1.96 and 0.39 indicate a range of crystallite sizes from small to large. This suggests that the material is affected by either mechanical or thermal stress, or even both. The crystallites in the material will be distorted and the size of the crystallite will be affected, resulting in a non-uniform microstructure.

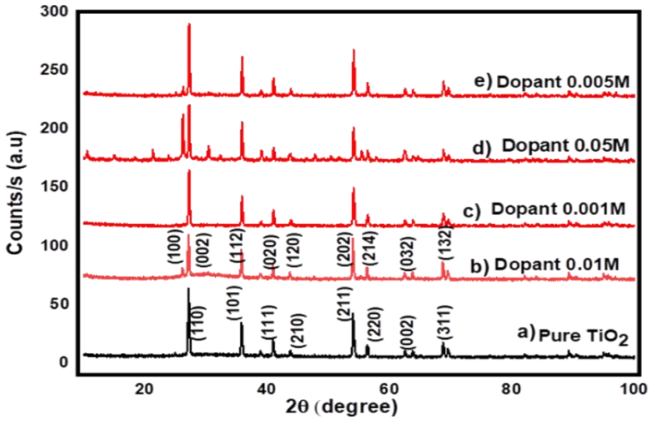

Fig.4. XRD analysis of Pure TiO_2 and TiO_2 doped with phosphomolybdic acid nanocomposite

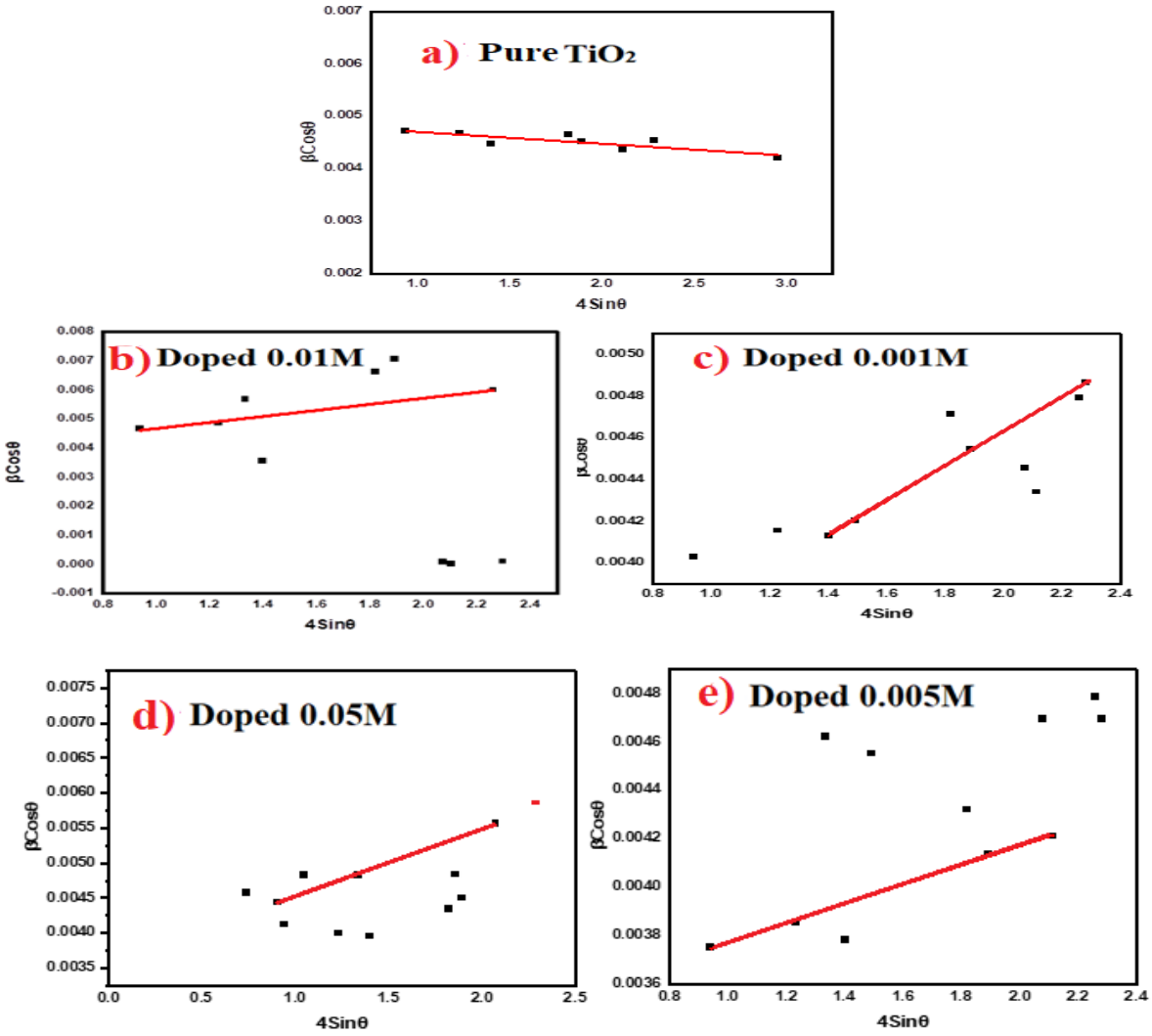

Fig.5. W-H Method plotting of (a) Pure TiO_2 and (b to e) TiO_2 doped with Phosphomolybdic acid nanocomposite samples

Table 2. W-H analysis of (a) Pure TiO_2 and (b to e) TiO_2 doped with Phosphomolybdic acid nanocomposite samples

Nano composites	Parameters		FWHM	intercept	Crystallite Size	Slope	Micro strain (ε)	d-spacing Average (Å)
	K	λ(Å)	β (°)	c=kλ/D	D(nm)	m		
Pure TiO_2	0.94	1.5406	0.2775	0.0037	29.63	0.0004	0.48	1.99
TiO_2 +PMA 0.01M	0.94	1.5406	0.2526	0.0036	37.30	0.0010	1.04	2.00
TiO_2 +PMA 0.001M	0.94	1.5406	0.2654	0.0020	32.86	0.0008	0.83	2.00
TiO_2 +PMA 0.05M	0.94	1.5406	0.4204	0.0035	33.69	0.0009	1.96	3.31
TiO_2 +PMA 0.005M	0.94	1.5406	0.2212	0.0033	42.97	0.0016	0.39	1.99

3.4 SEM and EDAX analysis

SEM images of sample 1 to 5 nanocomposites are shown in Fig. 5. TiO_2 metal exhibits a morphology which is almost spherically shaped, and micron-sized particles/grains[21]. These are secondary particles consisting of nano-sized primary particles, which are formed on agglomeration. Even the secondary particles have surface projected nano-size bristles-like structures, could be visualized in close view. Similarly the morphology of all samples Fig.6a to e nanocomposite are shown in these primary nano fringes. The EDAX results, shown in Fig.6a to e, confirm the presence of Ti, O, P and Mo elements in the nanocomposite, and proves that they are successfully doped with phosphomolybdic acid[22].

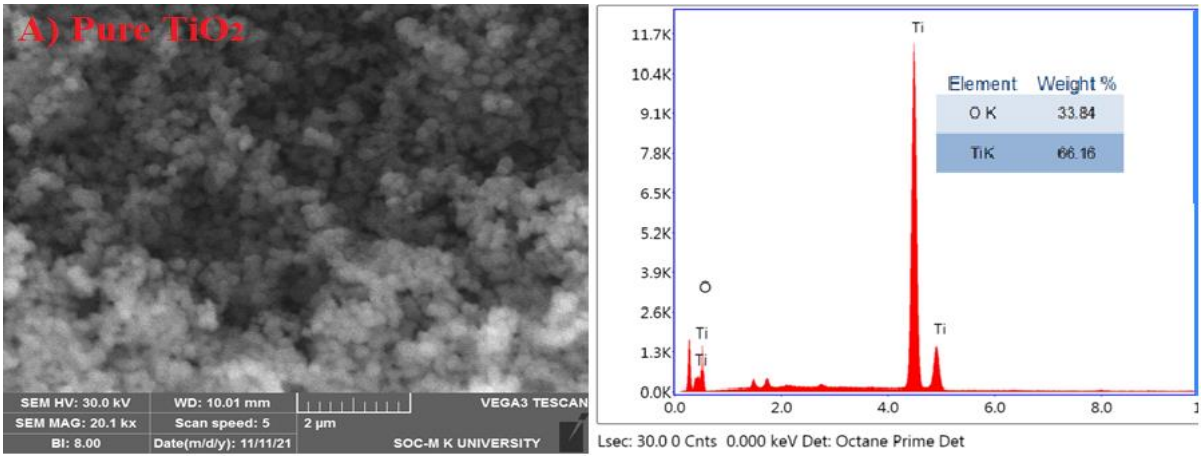

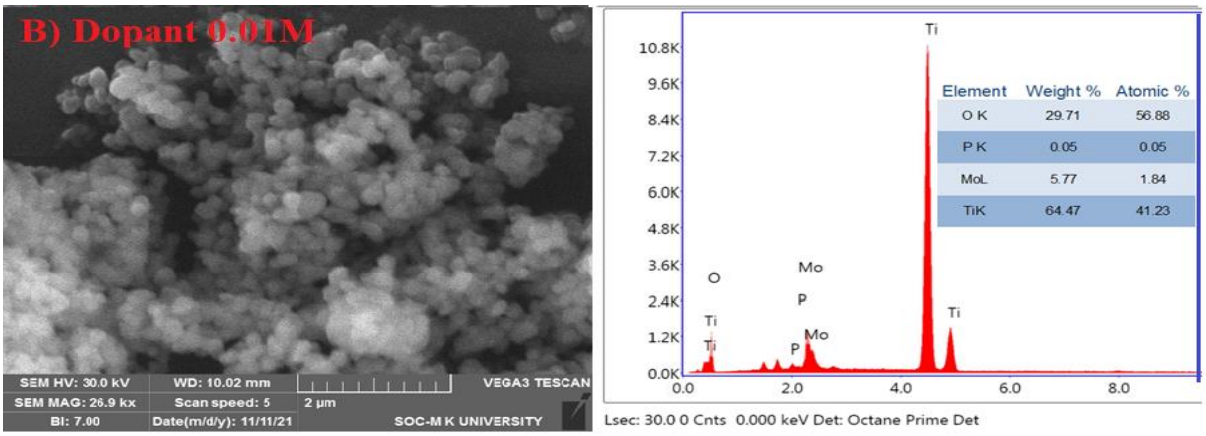

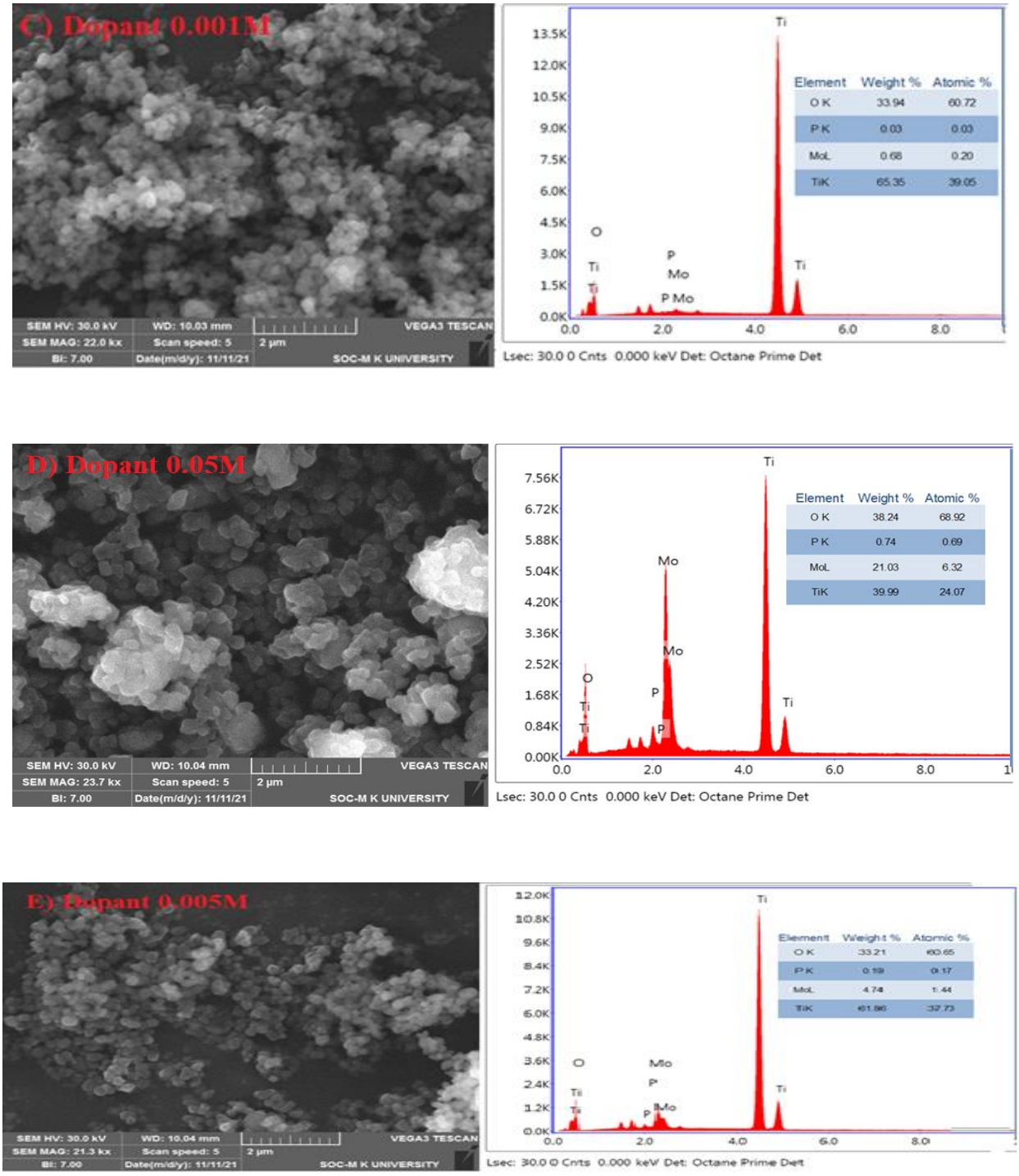

Fig.6. SEM and EDAX analysis of Pure TiO_2 and TiO_2 doped with phosphomolybdic acid nanocomposit

3.5 Map analysis

The images can be used to identify the presence of any impurities or other elements in the sample. The colour mapping can also be used to determine the size and distribution of the particles within the sample, as well as the distribution of the dopants. Additionally, the colour mapping can be used to analyze the surface topography of the sample, which can be useful in understanding the surface-level interactions between the sample and its environment. The map analysis was performed to investigate composites of TiO_2 doped phosphomolybdic acid. The results has been given in Fig.6. reveals the elemental composition and purity of the composite samples. The strong Titanium (Ti) and Oxygen (O) peaks were observed without any impurity, and confirmed by synthesized TiO_2 Fig.6a. The result dopant nanocomposite is in a good stoichiometric ratio[23]. The mapping analysis has been extended in Fig. 6b. The distribution of molybdenum is more uniform than that of phosphorus. Furthermore, molybdenum and phosphorus elements are well dispersed during in the composite preparation.

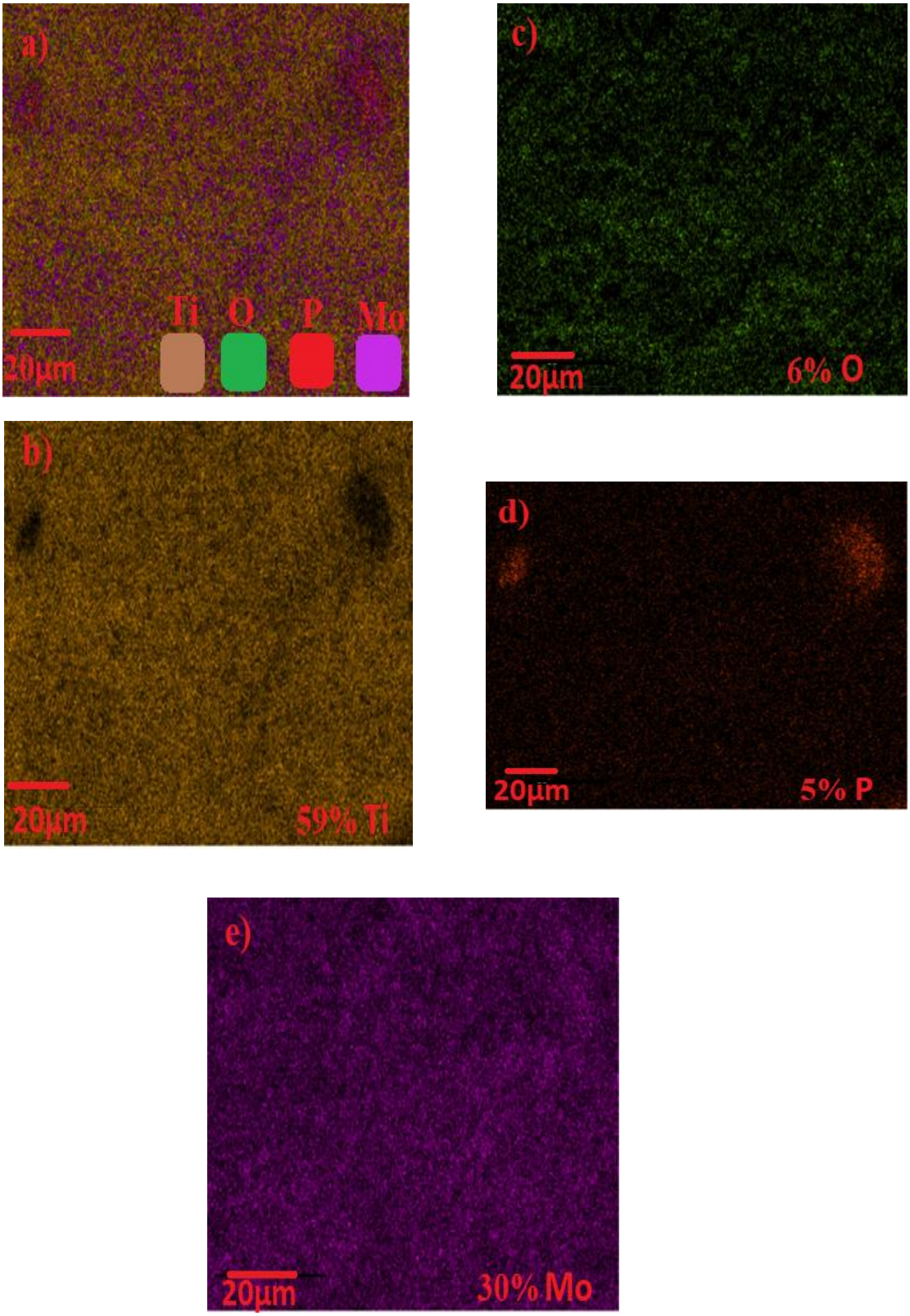

Fig.7. Elemental map analysis of (a) Pure TiO_2 and (b) TiO_2 doped with phosphomolybdic acid nanocomposite samples

3.6 Photocatalytic Studies

3.6.1 Photodegradation studies of methylene blue dye and airflow with catalyst

For the preliminary experiment, the photocatalytic degradation of methylene blue dye was carried out under conditions of constant airflow[24]. All these experiments were conducted at an initial methylene blue concentration

of 50 ppm and a catalyst dosage of 0.05M. In the preliminary experiments, and stabilized performance of photocatalyst (TiO_2 doped with phosphomolybdic acid) were investigated in the following conditions: absence of light,]Methylene blue dye] = 50ppm; Temp=33C; constant airflow and catalyst dosage of 0.05M. The results were shown in Fig.8. The % of degradation of methylene blue dye was found from 0 to 99% by varying minutes of the photocatalyst[25]. The TiO_2 doped with phosphomolybdic acid composites worked better under the condition of constant airflow than without airflow. In the absence of airflow, the surface of the nanocomposite was covered by a thin layer of pollutants, thereby reducing its photocatalytic activity. Dissimilarly, the results of the study revealed that the presence of airflow had a positive effect on the photodegradation of the methylene blue dyes

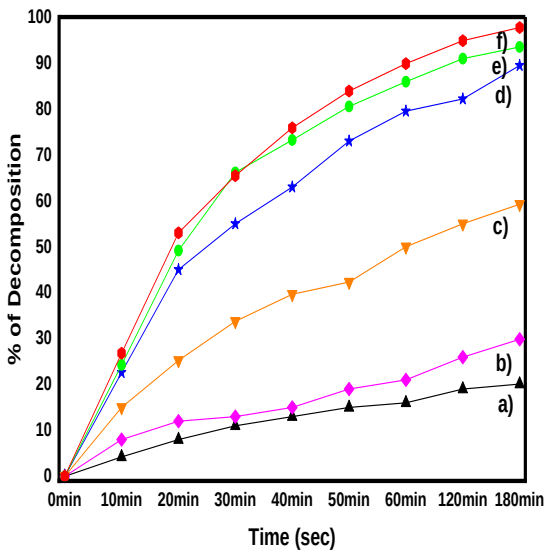

Fig. 8. Photocatalytic degradation of methylene blue with TiO_2 doped Phosphomolybdic acid photocatalyst concentration variation samples. a) 10mg b) 20mg c) 50mg d) 100mg e) 125mg f) 150mg

Condition: Methylene blue = 50 ppm; Temp = 33ºC; constant with/without airflow and Photodegradation wavelength = 365nm , UV absorbance = 460 nm

3.6.2 Effect of pH on photocatalytic degradation methylene blue

The effect of solution pH on the Methylene blue dye removal was plotted in Fig. 9. The pH was adjust, by the addition of 0.1M HCL and NaOH, at various pH values of 4, 6 and 8. After 60 min reaction obtained, of % degradation are, 90, 75, 32 respectively. The highest degradation efficiency was occurred at pH = 4 and the lowest degradation at pH 6 and 8. At highly acidic (pH 2 and 3), the surface of the catalyst is positive, since H can be attached to the metal TiO_2 group[26]. But, at pH 8 the catalyst surface may be negative. Since the pKa of methylene blue is high of pHs 4, and at lower pHs 6 and 8, the proportion of availability of aromatic ring in pH 4 will be increased higher. Eventually, pH 4 is a conducive condition for maximum adsorption of methylene blue. A similar observation of the values of pH conditions have been noted. Thus, at pH value 4, Methylene blue was degraded larger than at other pHs .

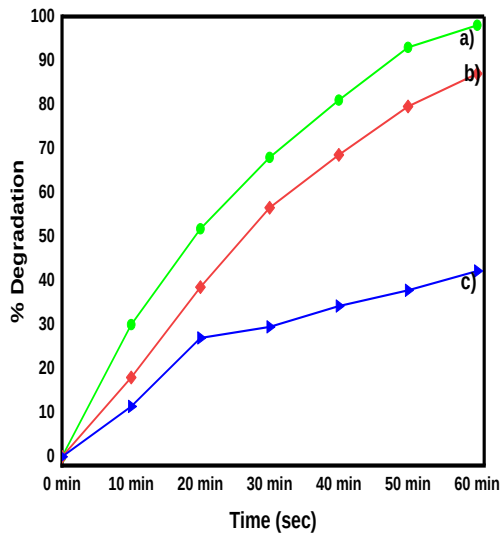

Fig. 9. Effect of pH variation on photodegradation of methylene blue samples a) 4 b) 6 c) 8

Condition: Methylene blue = 50 ppm; Temp = 33ºC; catalyst dose = 0.05M and constant without airflow and Photodegradation wavelength = 365nm, UV absorbance = 460 nm.

3.6.3 Effect of demineralization of Methylene blue dye

The photocatalytic degradation of Methylene blue under optimized condition: [MB=50 ppm], catalyst = 125mg, pH= 4 was studied using the synthesized composites under the visible light of wavelength 460nm, temp 33ºC; without airflow and dose of catalyst of 0.05M. Higher catalytic activity happened during the 2hr of reaction. After that, the catalysis occurred slowly but constantly. Finally the pollutant disappeared with in 4hrs. This dye is capable of absorbing a wide range of wavelengths, which makes it suitable for the photocatalytic oxidation of organic and inorganic compounds. Photocatalysis involves in the absorption of ultraviolet light by the dye, that leads to the formation of reactive oxygen species such as oxidize organic and inorganic compounds. The dye is also able to reduce the surface tension of water, and making it more conducive for complete demineralization. In addition, the photocatalytic effect of methylene blue dye can also be used to enhance the efficiency of existing water treatment technologies

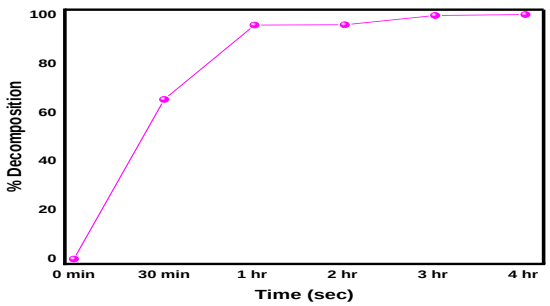

Fig. 10. Effect of demineralization of Methylene blue dye samples

Condition: Methylene blue = 50 ppm; Temp = 33ºC; catalyst dose = 0.05M and constant without airflow and Photodegradation wavelength = 365nm , UV absorbance = 460 nm

4. Antimicrobial Activity

Titanium dioxide (TiO_2) is a material that has been used to find that TiO_2 doesn't have antimicrobial activity. TiO_2 has been shown that it hasn't affect the growth of bacteria, fungi, and viruses, like *streptococcus pyogens MTCC 442*. Antimicrobial activity testing was carried out by using the Disc diffusion method agar method[27]. Each purified components that used in research, were dissolved in dimethyl sulfoxide (DMSO), sterilized by using a Petri plate, and stored at 4°C after incubating for 48hrs. For the determination of the zone of inhibition, pure Gram-positive, and Gram-negative, were taken as standard antibiotics for comparison after getting the results. Control experiments were carried out the condition by using amoxicillin clavulanate or clavulanic acid for antibacterial activity[28]. In Fig.10a, 1 is amoxicillin clavulanate or clavulanic acid an antibiotic and 2 is TiO_2 doped phosphomolybdic acid compound. The zones of growth around the disks were evaluate after 48 hours after incubation at 37°C. The antibacterial activity were confirmed in TiO_2 doped with phosphomolybdic acid. The results indicate that TiO_2 doped with phosphomolybdic acid has antimicrobial activity against a range of bacteria and fungi. Hence, it can be concluded that TiO_2 doped with phosphomolybdic acid has no antimicrobial activity against Streptococcus pyogenes MTCC 442.

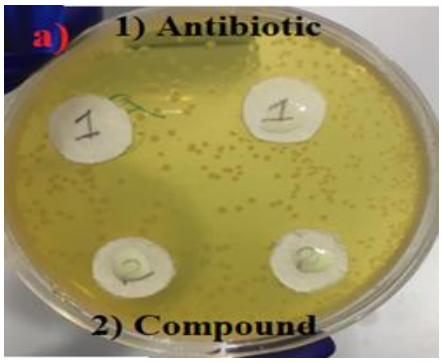

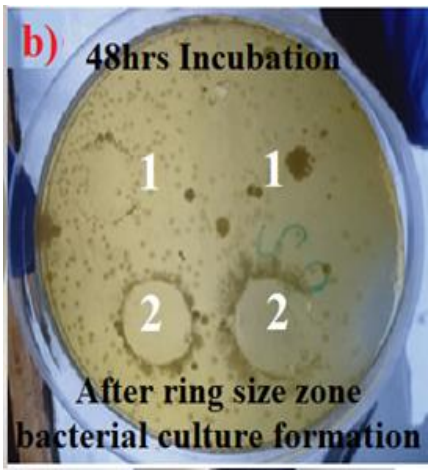

Fig.11 Antimicrobial activity of TiO_2 doped with phosphomolybdic acid nanocomposite samples

Acknowledgement

The authors are thankful for St. John's College, Palayamkottai, Tirunelveli, India; for furnishing necessary provision and support for this work.

References

[1] Siadati, Seyyed A mir, Esmail Vessally, Akram Hosseinian, and Ladan Edjlali. "Possibility of sensing, adsorbing, and destructing the Tabun-2D-skeletal (Tabun nerve agent) by C20 fullerene and its boron and nitrogen doped derivatives." *Synthetic Metals* 220 (2016): 606-611.

[2] E Bet-*moushoul*, Y Mansourpanah, Kh Farhadi, Tabatabaei M. TiO_2 nanocomposite based polymeric membranes: A review on performance improvement for various applications in chemical engineering processes. *Chem. Eng. Journal*. (2016). 0283:29–46.

[3] Vessally, Esmail, Seyyed Amir Siadati, Akram Hosseinian, and Ladan Edjlali. "Selective sensing of ozone and the chemically active gaseous species of the troposphere by using the C20 fullerene and graphene segment." *Talanta* 162 (2017): 505-510

[4] Li, Shuang, Yingai Li, Hao Chen, Youzhi Yang, Yanhong Lin, and Tengfeng Xie. "N-Doped TiO_2 Coupled with Manganese-Substituted Phosphomolybdic Acid Composites As Efficient Photocatalysis-Fenton Catalysts for the Degradation of Rhodamine B." *Langmuir* 38, no. 50 (2022): 15817–26.

[5] Colombo Migliorero, M. B., Palermo, V., Romanelli, G. P., & Vázquez, P. G. Niobium-doped phosphomolybdic acid catalyst included in silica matrix: Study of stability and reactivity using different loads. *Latin American Applied Research - An International Journal*, 53(1), (2023). 49–54.

[6] Jin, X.-Y., Zhao, J., Ge, Q., Jiang, N., Liu, M., Cong, H., & Zhang, Y.-Q.. Carbon nanomaterials made from supramolecular hybridization of cucurbit[6]uril with phosphomolybdic acid for supercapacitors. *ACS Applied Nano Materials*, (2023) 6(4), 2459–2471.

[7] V Rodríguez, R Camarillo, F Martínez, C Jiménez, J Rincon. CO_2 photocatalytic reduction with CNT/TiO_2

based nanocomposites prepared by high-pressure technology. *The Journal Super. Fluids*. (2020). 163:104876

[8] Waris, A. Hakeem Anwer, F. Abdulaziz, S. Latif, A. Alanazi, S. Sultana, M. Zain Khan, Microwave assisted green synthesis of high capacitive TiO_2 doped rGO nanosheets for supercapacitor applications, *Materials Science and Engineering: B*. 291 (2023) 116367.

[9] Y Yulizar, Sudirman, DOB Apriandanu, AP Wibowo. Plant extract mediated synthesis of Au/TiO_2 nanocomposite and its photocatalytic activity under sodium light irradiation. *Composites Comm*. (2019). 16:50–56

[10] AS Montaser, R Wassel Ahmed, ON Al-Shaye'a.. Synthesis, characterization and antimicrobial activity of Schiff bases from chitosan and salicylaldehyde/TiO_2 nanocomposite membrane. *International Journal Bio. Macro*. (2019) 124:802–9

[11] S Alkaykh, A Mbarek, EE Ali-Shattle. Photocatalytic degradation of methylene blue dye in aqueous solution by $MnTiO_3$ nanoparticles under sunlight irradiation. *Heliyon*. (2020). 6(4) e03663

[12] X. Feng, L. Gu, N. Wang, Q. Pu, G. Liu, Fe/N co-doped nano-TiO2 wrapped mesoporous carbon spheres for synergetically enhanced adsorption and photocatalysis, *Journal of Materials Science & Technology*. 135 (2023) 54–64.

[13] P.S. Koujalagi, H.N. Revankar, V.R. Gurjar, R.M. Kulkarni, Adsorption of Chromium (VI) from Aqueous Solution Using Nano TiO_2 Doped Strong Base Anion Exchange Resin, *CNM*. 8 (2023) 397–408.

[14] D Sharma, M Kumari, V Dhayal. Fabrication and characterization of cellulose/PVA/TiO_2 nanocomposite thin film as a photocatalyst. *Materials Today: Proceedings*. (2021). 43:2970–74

[15] J.E., Madhusree, Chandewar, Pranay R., Shee, Debaprasad, & Sankar Mal, Sib.. Phosphomolybdic acid embedded into biomass-derived biochar carbon electrode for supercapacitor applications. *Journal of Electroanalytical Chemistry*, (2023). *936*, 117354.

[16] Jin, Xian-Yi, Zhao, Jie, Ge, Qingmei, Jiang, Nan, Liu, Mao, Cong, Hang, & Zhang, Yun-Qian.. Carbon nanomaterials made from supramolecular hybridization of cucurbit[6]uril with phosphomolybdic acid for supercapacitors. *ACS Applied Nano Materials*, (2023)6(4), 2459–2471.

[17] F. Arjomandi Rad, J. Talat Mehrabad, Structural and Optical Properties Study of Ag and Mg co-Doped TiO_2 by Comparison between DFT Calculation with Experimental Results, International Journal of Nanoscience and Nanotechnology. 19 (2023).

[18] S Sambaza, A Maity, K Pillay. Enhanced degradation of BPA in water by PANI supported Ag/TiO_2 nanocomposite under UV and visible light. *J. Env. Chem. Engineering*. (2019). 7(1):102880

[19] I.Baragau, J. Buckeridge, K.G. Nguyen, T. Heil, M.T. Sajjad, S.A.J. Thomson, A. Rennie, D.J. Morgan, N.P. Power, S.A. Nicolae, M.-M. Titirici, S. Dunn, S. Kellici, Outstanding visible light photocatalysis using nano-TiO_2 hybrids with nitrogen-doped carbon quantum dots and/or reduced graphene oxide, J. Mater. Chem. A. 11 (2023) 9791–9806.

[20] S Mustapha, JO Tijani, MM Ndamitso, AS Abdulkareem, DT Shuaib et al. Facile synthesis and characterization of TiO_2 nanoparticles: X-ray peak profile analysis using Williamson–Hall and Debye–Scherrer methods. *Int Nano Lett*. (2021). 11(3):241–61

[21] S Magar, GT Mohanraj, SK Jana, CV Rode. Synthesis and characterization of supported heteropoly acid: Efficient solid acid catalyst for glycerol esterification to produce biofuel additives. *In. Nano-Metal Chemistry*. (2020). 50(11):1157–65

[22] A. Haghighizadeh, A. Aghababai Beni, M. Haghmohammadi, M.S.S. Adel, S. Farshad, Green Synthesis of ZnO-TiO_2 Nano-Photocatalyst Doped with Fe(III) Ions Using Bitter Olive Extract to Treat Textile Wastewater Containing Reactive Dyes, Water Air Soil Pollut. 234 (2023) 366.

[23] K Divakaran, A Baishnisha, V Balakumar, KN Perumal, C Meenakshi, RS Kannan. Photocatalytic degradation of tetracycline under visible light using TiO_2@sulfur doped carbon nitride nanocomposite synthesized via in-situ method. *J. Env. Che. Engineering*. (2021). 9(4):105560

[24] M Aravind, M Amalanathan, MSM Mary, C Parvathiraja, AA Alothman et al. Enhanced Photocatalytic and Biological Observations of Green Synthesized Activated Carbon, Activated Carbon Doped Silver and Activated Carbon/Silver/Titanium Dioxide Nanocomposites. *J Inorg Organomet Polym*. (2022). 32(1):267–79

[25] Y Wang, X Liu, L Guo, L Shang, S Ge et al. Metal organic framework-derived C-doped ZnO/TiO_2 nanocomposite catalysts for enhanced photodegradation of Rhodamine B. *J. Colloid and Interface Sci*. (2021). 599:566–76

[26] F Iazdani, A Nezamzadeh-Ejhieh. Supported cuprous oxide-clinoptilolite nanoparticles: Brief identification and the catalytic kinetics in the photodegradation of dichloroaniline. *Spectrochimica Acta Part A: Mole. and Bio. Spectroscopy*. (2021). 250:119348

[27] P Dong, F Yang, X Cheng, Huang Z, Nie X, et al. Plasmon enhanced photocatalytic and antimicrobial activities of Ag-TiO_2 nanocomposites under visible light irradiation prepared by DBD cold plasma treatment. *Mat. Sci and Engineering: C*. (2019). 96:197–204

[28] M Mesgari, AH Aalami, A Sahebkar. Antimicrobial activities of chitosan/titanium dioxide composites as a biological nanolayer for food preservation: A review. *I. Journal Bio. Macro*. (2021). 176:530–39